Available online at www.sciencedirect.com
SCIENCE DIRECT®
Journal of Solid State Chemistry 173 (2003) 359–366
JOURNAL OF SOLID STATE CHEMISTRY
http://elsevier.com/locate/jssc

Defect chemistry and VUV optical properties of the $BaMgAl_{10}O_{17}:Eu^{2+}$–$Ba_{0.75}Al_{11}O_{17.25}:Eu^{2+}$ solid solution

Valerie Pike,[a] Samuel Patraw,[a] Anthony L. Diaz,[a,*] and Barry G. DeBoer[b]

[a] *Department of Chemistry, Central Washington University, Ellensburg, WA 98926, USA*
[b] *RR1 Box 586, Ulster, PA 18850, USA*

Received 14 October 2002; received in revised form 27 January 2003; accepted 13 February 2003

Abstract

The optical properties of the $BaMgAl_{10}O_{17}:Eu^{2+}$ (BAM)–$Ba_{0.75}Al_{11}O_{17.25}:Eu^{2+}$ (BAL) solid solution have been studied using VUV excitation, emission and reflectance spectroscopy. Three unique Eu^{2+} emission centers are observed in a ratio that depends on the composition of the host and the dopant concentration. Two of the emission centers are assigned to Eu on normal Beevers–Ross sites and Eu on anti Beevers–Ross sites. The defect chemistry of this system is modeled based on the known behavior of the spinel ($MgO \cdot nAl_2O_3$) system. Based on this model, the third Eu center can be assigned either to Eu near Al vacancies or to Eu associated with O atoms in the cation layer. In undoped materials exciton emission is observed, peaking at 263 nm in BAM and 285 nm in BAL. This emission may be the mechanism of host-to-activator energy transfer in these phosphors.
© 2003 Elsevier Science (USA). All rights reserved.

Keywords: BAM; Luminescence; VUV; Hexaaluminates; Eu^{2+}

1. Introduction

$BaMgAl_{10}O_{17}:Eu^{2+}$ (BAM) is the blue phosphor component of three-color fluorescent lamps and plasma display panels (PDP). Fabrication of a PDP involves a binder burn-off step that exposes the phosphors to temperatures of 450–550°C in the presence of oxygen. This leads to a significant decrease in the radiant efficiency of BAM as a result of oxidation of Eu^{2+} to Eu^{3+} [1,2]. In addition, a PDP achieves excitation of the phosphor layer via a Xe plasma discharge that generates vacuum ultraviolet (VUV) radiation at 147 and 172 nm. After long exposures to this radiation, however, BAM exhibits further loss of efficiency, as well as a color shift [3,4]. The color shift is apparently the result of the formation of a new Eu^{2+} emission center. This new emission has been fitted to a peak at around 493 nm that adds a shoulder to the usual BAM emission at 450 nm [5]. Presently, the mechanisms behind these damage processes are not well understood. However, there is increasing evidence that the solid solution between BAM and $Ba_{0.75}Al_{11}O_{17.25}:Eu^{2+}$ (BAL) can significantly influence the VUV and thermal stability of this material. Thus, study of this solid solution may provide some important insight into the relationships between structure and stability in BAM.

The ternary phase diagram for the BaO–MgO–Al_2O_3 system was reported by Göbbels et al. [6] and a slight modification has been proposed by Diaz et al. [1]. BAM and BAL are hexaaluminates that form with the β-alumina structure in space group $P6_3/mmc$. The structure of BAM consists of $MgAl_{10}O_{16}$ spinel-like units with intervening Ba–O layers [7]. A complete solid solution exists between the 1:1:5 phase, $BaMgAl_{10}O_{17}$, and a phase with the stoichiometry of BAL. However, replacement of Mg^{2+} ions with Al^{3+} requires that some modest structural rearrangement take place to compensate for the additional positive charge. Single-crystal X-ray studies on BAL indicate that some of the Ba in the cation layer is replaced by O atoms, with a corresponding migration of Al atoms to form Al_i–O_{Ba}–Al_i bridges between the spinel blocks (where Al_i denotes an interstitial Al atom and O_{Ba} is an oxygen atom on a Ba site) [8,9]. This creates additional links between spinel layers that are randomly distributed throughout the crystal lattice. This conclusion is also supported by some recent theoretical calculations [10].

Compositional changes along the BAM–BAL solid solution have a profound influence on the optical properties of doped Eu^{2+}. Under 254 nm excitation,

*Corresponding author.
E-mail address: diaza@cwu.edu (A.L. Diaz).

0022-4596/03/$ - see front matter © 2003 Elsevier Science (USA). All rights reserved.
doi:10.1016/S0022-4596(03)00111-7

BAM:Eu^{2+} exhibits a single emission band centered at 450 nm. BAL:Eu^{2+} exhibits a much broader emission spectrum, with the appearance of at least one new emission center at wavelengths longer than 450 nm. BAL also has additional lower energy excitation peaks. These changes grow in steadily with changes in composition along the join. Previously, the new emission in BAL has been assigned to Eu^{2+}–O_{Ba} associates [11] or to Eu^{2+} atoms in cation sites within the spinel block [12,13]. Interestingly, this new emission is centered at nearly the same wavelength as is observed in BAM that has been damaged by VUV radiation [5]. Jüstel and Nikol, in fact, have previously made this association, and suggest that the use of excess Mg^{2+} during the synthesis of BAM leads to improved VUV stability because it prevents the formation of compositions away from the ideal 1:1:5 [14]. Diaz et al. also found that as the composition of the phosphor is changed from BAM to BAL, the phosphors exhibit poorer thermal stability with respect to color and brightness [1]. On the other hand, Yokota et al. have proposed the opposite—that compositions along the solid solution join are more thermally stable [15]. Zhang et al. have also claimed an improvement in VUV stability with off-stoichiometry compositions [5]. Clearly, additional research on the behavior of these compounds is required to clarify these discrepancies.

Even though there is only a single crystallographically unique Ba site in these structures, several researchers have recently proposed that there are actually two or three distinct Eu^{2+} emission centers in doped stoichiometric BAM. Evidence for this comes from ^{151}Eu Mössbauer spectroscopy [16], theoretical modeling of Eu^{2+} excitation spectra [17] and from studies of Sm^{2+} emission in $BaMgAl_{10}O_{17}$ [18]. These sites have been assigned to Eu on the normal Ba site (the Beevers–Ross site), to Eu displaced onto anti-Beevers–Ross sites and to Eu on mid oxygen sites in the cation layer. None of these studies were extended to include the BAM–BAL solid solution.

The results presented here constitute the beginning of an extensive investigation into the relationships between the defect chemistry, optical properties and radiation damage behavior of BAM. We have chosen to initiate this work with a VUV spectroscopic study of the BAM–BAL solid solution. The purpose of the work presented here is to shed further light on the number and nature of emission centers in these materials, and to correlate the solid solution defect chemistry with specific changes in VUV optical properties. Ultimately, this knowledge will be applied to a study of the mechanisms behind thermal and radiation damage in BAM.

2. Experimental

Samples along the BAM–BAL solid solution join were prepared by wet ball-milling of blends of $BaCO_3$, $Al(OH)_3$, MgO, and Eu_2O_3. A small amount of BaF_2 was used in place of $BaCO_3$ as a reaction aid. The samples were twice fired for 3 h in open alumina crucibles under a 75% H_2/25% N_2 flow at 1650°C, with milling between firing steps. Samples were analyzed by glow discharge mass spectroscopy to check that no F was retained. Samples were analyzed for phase purity using a Philips PW3400 automated powder X-ray diffractometer. All samples were found to be single phase.

Spectra were obtained using a deuterium lamp attached to a VUV monochromator (Acton Research Corporation, VM 502) for excitation, and an ARC SP-150 UV/Vis monochromator with PMT for measuring sample emission. Powder samples mount vertically in the chamber at 60° in, 30° out. The lamp, excitation monochromator and sample chamber are evacuated using a diaphragm/turbomolecular pumping station (Pfeiffer Vacuum, TSU 071E), to a base pressure of 5.4×10^{-5} mbar. The system provides usable excitation radiation between about 125 and 300 nm. Excitation spectra were corrected using a sodium salicylate standard, while emission spectra were corrected using a NIST calibrated standard lamp (Oriel, Model #63355). By comparing the VM 502 throughput with and without a 3/8″ CaF_2 window (which begins to absorb below about 150 nm), we determined that second order throughput of wavelengths between 125 and 150 nm accounts for less than 5% of the observed intensity between 250 and 300 nm. As a result, we chose not to correct for this effect.

For reflectance measurements, the instrument above was re-configured as shown in Fig. 1. The sample chamber was placed between the light source and the VUV monochrometer at an incident angle of 60° (to avoid specular reflection). A PMT with a sodium salicylate coated window was used as the detector in this configuration. With this approach, all wavelengths

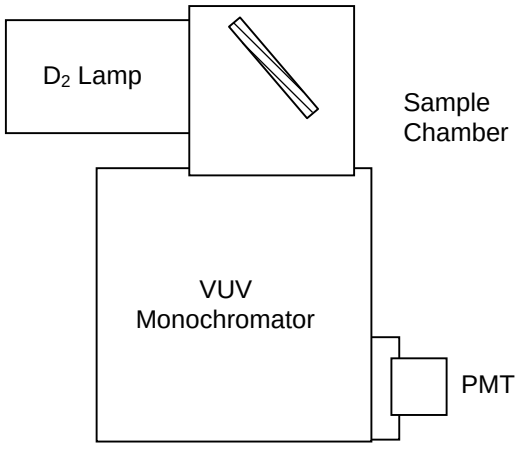

Fig. 1. Schematic of the configuration used to measure reflectance from powder samples.

are incident on the sample simultaneously, and wavelength selection is done after reflection from the sample surface. The spectra are corrected using MgF_2 as a standard between 125 and 300 nm. It was necessary to attenuate the lamp intensity using a piece of sheet tin with a hole in it. Ideally, a reflectance measurement would be done using a synchronous scan of two VUV monochromators. However, this method proved effective and is much simpler than the approach described recently by Wiechert and co-workers [19]. Its primary limitation is the inability to filter out second order throughput, but, as stated above, this effect was small enough that it did not significantly affect the outcome of the measurement.

3. Results and discussion

3.1. VUV emission, excitation and reflectance spectra

The BAM–BAL compositional join can be described algebraically in several ways. In this work, we describe the system such that the composition of the spinel block is considered separately from the cation layer. Justification for this approach is provided later in the text (under *Defect Chemistry of the β-aluminates*). The end points of the solid solution are then $BaO \cdot MgAl_{10}O_{16}$ and $0.727BaO \cdot Al_{10.67}O_{16}$, and the join is described by the equation

$$(1 - \tfrac{3}{11}x)BaO \cdot Mg_{1-x}Al_{10+(2/3)x}O_{16}. \quad (1)$$

Throughout this paper, the compositional variable "x" is in reference to Eq. (1).

In Fig. 2, emission spectra under 147 nm excitation are shown for BAM, BAL and the composition given by $x = 0.51$. The Eu doping level in these samples is 10 mol%. The spectra shown here are essentially identical to those reported by Smets and Verlijsdonk for 254 nm excitation [13]. Pure BAM exhibits a broad emission band centered at 448 nm. As the composition changes the emission band broadens and extends out to 680 nm, clearly indicative of a change in the number and nature of Eu^{2+} emission centers in the host. In addition, the integrated intensity of the emission of BAL is only about 65% that of BAM.

Excitation spectra are shown in Fig. 3 for the same compositions. The emission wavelength is 450 nm. Excitation at wavelengths longer than about 210 nm corresponds to direct excitation of the Eu activator, while excitation below 210 nm corresponds to excitation through the host. Host excitation in the VUV is characterized by peaks at about 155 and 170 nm. An additional peak at 205 nm appears as the composition changes from BAM to BAL. Excitation in the UV occurs as a broad band. Although not shown, this band extends out to about 400 nm in BAM and to about 490 nm in BAL [11–13]. The small fluctuations between 230 and 280 arise from second order throughput of the VUV monochromator, as described in the Experimental section. Note that excitation between 150 and 175 nm provides more light output than excitation into the highest-lying Eu levels.

Absorption spectra of BAM and BAL, doped at 10 mol% Eu^{2+}, are shown in Fig. 4. The y-axis scale is 1 minus the reflectance $(1 - r)$ relative to MgF_2. Both spectra essentially mimic the excitation spectra. The spectrum of BAM shown here is essentially the same as that reported by Wiechert and co-workers [19]. BAL exhibits less absorption than BAM between 180 and 240 nm, revealing a peak at about 209 nm. The absorption and excitation spectra indicate that the relative quantum efficiency of BAM is slightly greater at 160 nm than at 254 nm.

Our attempts to obtain reflectance data on undoped material produced unusual results, in that we were finding additional light output (i.e., corrected reflectances with values above 1.0) in the 210–300 nm wavelength range. The authors believe that this

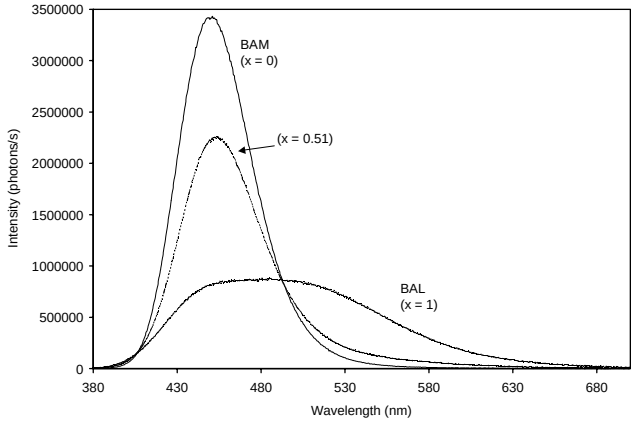

Fig. 2. Emission spectra of Eu^{2+}-doped compositions on the BAM–BAL join ($\lambda_{ex} = 147$ nm).

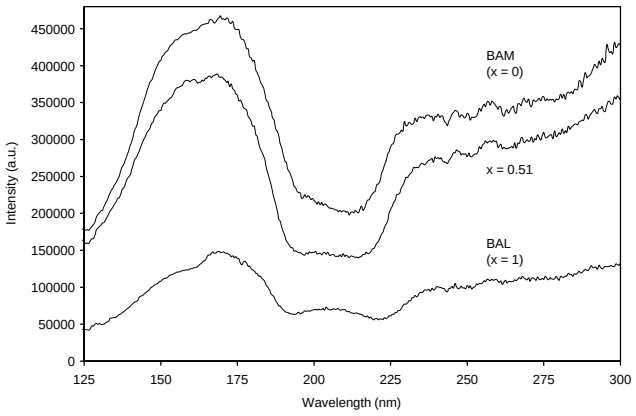

Fig. 3. Excitation spectra at $x = 0$ (BAM), $x = 0.51$ and $x = 1.0$ ($\lambda_{em} = 450$ nm).

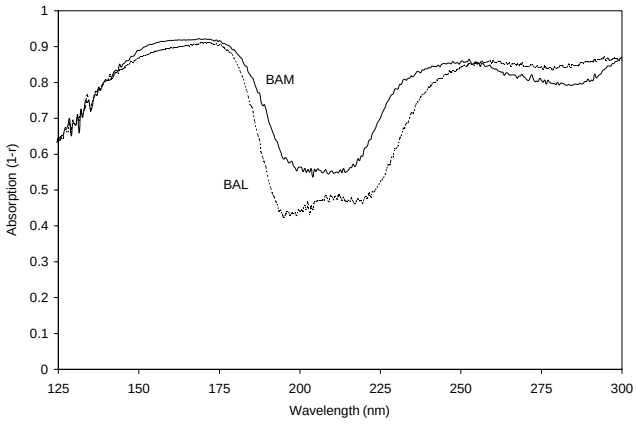

Fig. 4. Absorption spectra of BAM (solid line) and BAL (dashed line) doped at 10 mol% Eu^{2+}.

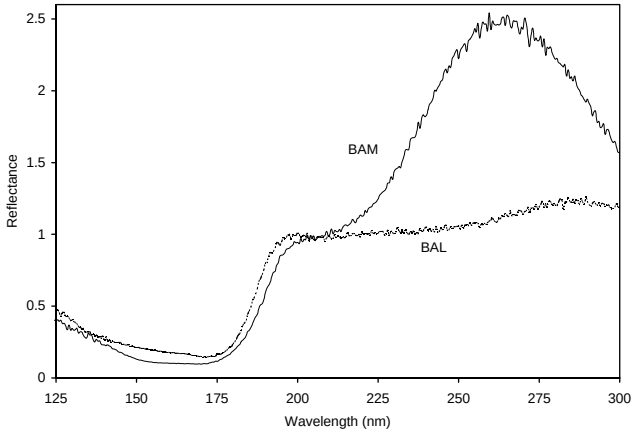

Fig. 5. Reflectance spectra of undoped BAM and BAL relative to MgF_2.

phenomenon is the result of exciton emission from the host. The spectra are shown in Fig. 5. The *y*-axis in this figure is a reflectance scale relative to MgF_2. In undoped BAM, a broad peak appears with a maximum at 263 nm. In BAL, the peak is shifted to 285 nm and is less intense. Note that in our experimental setup for reflectance, all wavelengths are incident on our sample simultaneously; wavelength selection occurs after the sample. Thus, radiation incident on the samples between 115 and 190 nm results in the emission that we detect at longer wavelengths. These emissions were detected directly in a second measurement using our emission spectrometer fit with a different grating. Because the optics are not designed for the detection of such short wavelengths, the signal was quite weak, and the spectra are not shown here.

From these spectra, the band edge (estimated by the onset of host absorption) occurs at about 190 nm (52,080 cm^{-1} or 6.46 eV) in BAL and 194 nm (51,550 cm^{-1} or 6.39 eV) in BAM. The calculated Stokes shifts for the exciton emission are then 13,530 cm^{-1} in BAM and 16,990 cm^{-1} in BAL. Such data have not been previously reported for these materials, but the Stokes shifts are in reasonable agreement with values obtained for host-lattice emission from tantalates and niobates, which exhibit Stokes shifts in the range of 10,000–15,000 cm^{-1} [24]. The authors note that this emission is not observed in samples doped at 10% Eu. We believe that this, together with the virtually identical emission spectra of Eu^{2+} doped samples under VUV and UV excitation, is strong evidence of host-lattice emission as the mechanism of energy transfer to Eu^{2+} in BAM. We also point out that in these spectra, apparent reflectance values greater than 2 do not imply multi-photon emission—the incident deuterium lamp spectrum has a strong band at $\sim$160 nm that is much more intense than the continuum in the region of the exciton emission.

Normalized excitation spectra of this emission in undoped BAM and BAL are shown in Fig. 6. The signal of the emission is relatively weak at 315 nm (the short wavelength limit of the emission optics), so the spectra are somewhat noisy. Note that the excitation is consistent with the band structures that are seen in the reflectance spectra of these compounds. We regard this as further evidence that the emissions detected from these materials correspond to radiative relaxation of an excited state in the host. Undoped BAM exhibits two excitation peaks at 153 and 166 nm. In BAL, the intensity of the peak at 153 nm decreases relative to a new shoulder at about 180 nm. Without firm theoretical models for such phenomena, it is difficult to make specific assignments for the peaks in the excitation spectra. At this point, we can only say that the change in composition leads to subtle changes in the band structure, as well as to a larger Stokes shift of the exciton emission. In addition, it appears that the efficiency of this emission is greatly reduced in BAL, possibly because of the introduction of new vacancies and other defects in the structure of BAL relative to

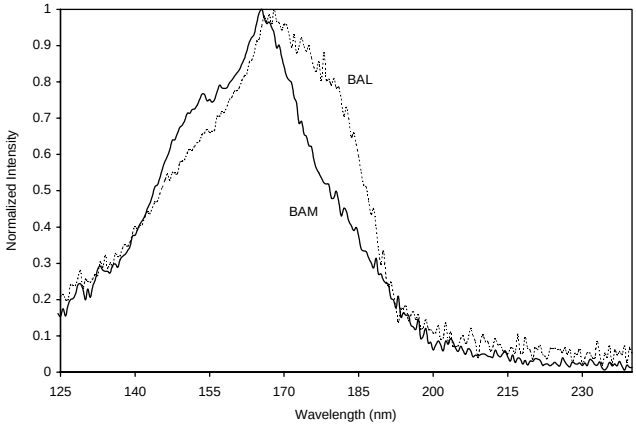

Fig. 6. Normalized excitation spectra of undoped BAM and BAL ($\lambda_{em} = 315$ nm).

that of BAM. This may explain the reduced efficiency of Eu-doped BAL under VUV excitation.

3.2. Characterization of Eu^{2+} emission centers

In order to clarify the assignment of the emission centers in these hosts we have fit the Eu^{2+} emission spectra for a series of compositions using Gaussian profiles. This approach comes from the configurational coordinate model, which predicts that the Frank–Condon overlap between ground and excited states will produce a Gaussian lineshape in a plot of photon number versus photon energy [20,21]. Previously, Ellens et al. used Gaussians to fit the emission spectra of Sm^{2+} in BAM [18], and determined that there are at least two unique Eu sites. Our best fits of the normalized Eu emission spectra of BAM and BAL using three Gaussian lines are shown in Figs. 7 and 8, respectively. In the case of BAL, the spectrum cannot reasonably be fit with two centers, so three are used. In BAM, the lowest energy peak is present with a very low intensity. However, this peak grows in smoothly with composition, so three lines were used to fit all of the data. Fits using these centers were carried out at eight compositions between BAM and BAL. It should be noted that during the course of the fitting the peak positions were allowed to vary, but they remained constant to within 5%. Peak widths increased smoothly with composition. The peaks occur at 448 nm (22,250 cm^{-1}), 475 nm (21,100 cm^{-1}) and 538 nm (19,000 cm^{-1}) and are labeled EuI, EuII and EuIII, respectively. In keeping with the assignments of Boolchand et al. [16] and Mishra et al. [17], we assign EuI to Eu^{2+} on a normal Ba site in the BAM lattice (Beevers–Ross or BR site), and EuII to Eu^{2+} displaced to an anti-Beevers–Ross (anti-BR) site. The assignment of EuIII is discussed below.

The peak fitting data for all of the compositions are summarized in Fig. 9. Here, the relative areas of each peak (as a percentage of the total integrated emission)

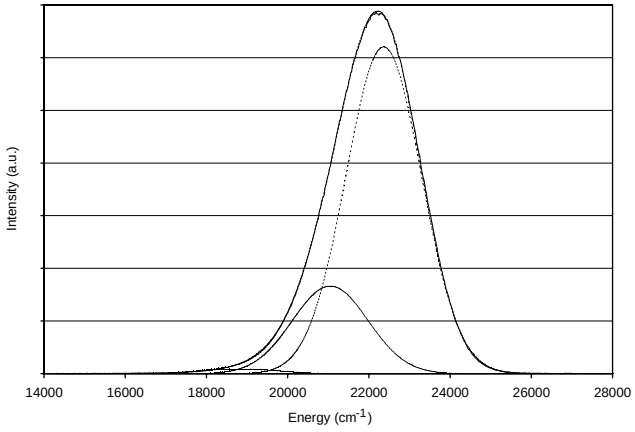

Fig. 7. Normalized emission spectrum of BAM fit to three Gaussians (excitation at 147 nm).

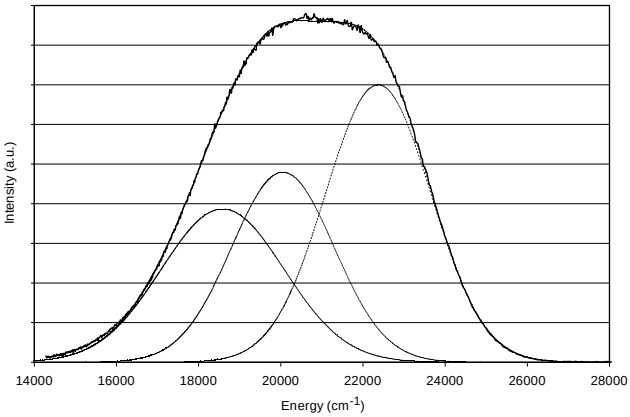

Fig. 8. Normalized emission spectrum of BAL fit to three Gaussians (excitation at 147 nm).

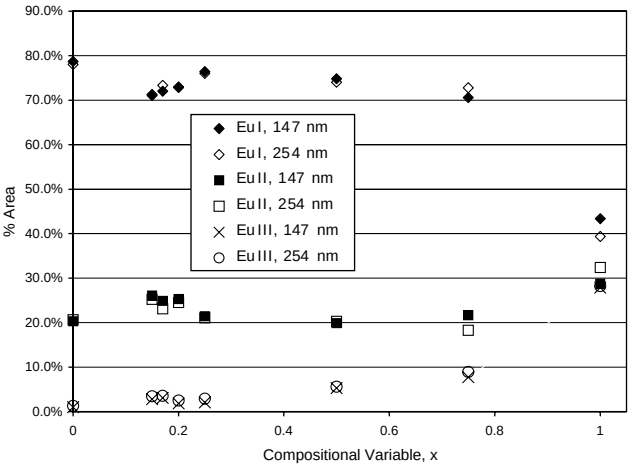

Fig. 9. Relative intensities of the three emission centers in the BAM–BAL solid solution, under 147 and 254 nm excitation.

are plotted as a function of the compositional variable x described in Eq. (1). Fits were done separately for emission spectra under 147 nm and 254 nm excitation. EuIII increases from 1% to 29% of the total emission as x goes from 0 to 1, and appears to replace the EuI center as the composition changes. EuII remains essentially unchanged, although it may increase slightly at $x = 1$ (BAL). It is important to note that there is essentially no difference in the emission spectra between 147 and 254 nm excitation. This is consistent with the hypothesis that energy transfer takes place via exciton emission. If the transfer mechanism were dependent on the local Eu^{2+} coordination environments it seems likely that there would be differences in the relative intensities of the emission centers under the two exciting wavelengths.

3.3. Defect chemistry of the β-aluminates

While the assignment of the EuI and EuII emission centers is relatively clear, the assignment of the EuIII

emission is more difficult. As discussed above, this center has been assigned to Eu–O_{Ba} pairs, to Eu in the spinel block, and more recently to Eu at mid-oxygen sites in the cation plane [17]. The assignment of Eu–O_{Ba} pairs is based on the crystal structure of BAL, whereas the other assignments are more speculative. Here, we discuss the assignment based on a detailed consideration of the defect chemistry of the BAM–BAL solid solution.

Our model of this system stems from an analysis of the defect behavior of spinel compositions, $MgO \cdot nAl_2O_3$. The spinel structure consists of close-packed oxygen layers, with Mg^{2+} in tetrahedral sites and Al^{3+} in octahedral sites. Excess alumina is soluble in spinel up to about $n = 2.5$, depending on the temperature [6]. The replacement of Mg^{2+} with Al^{3+} requires that Al^{3+} vacancies be created elsewhere in the lattice for charge balance. The defect chemistry of the spinel solid solution has been discussed in detail by Gritsyna et al. who derived a simple expression for the site occupancy in spinel as additional Al is added to ideal $MgAl_2O_4$ [22]

$$(Mg_{1-y}Al_y)^{IV}(Al_{2-y/3}\square_{y/3})^{VI}O_4. \quad (2)$$

Here, additional Al atoms replace Mg in tetrahedral sites (labeled IV) and 1/3 of an octahedral vacancy (denoted with a "□") is created for charge balance.

BAL has traditionally been described on an Al = 11.0 basis, i.e., as the addition of one more Al atom to replace Mg in the BAM lattice. An alternative approach is to describe the compositions along the BAM–BAL join with a model in which the oxygen lattice in the spinel layer is not disrupted along the solid solution. In other words, the replacement of Mg^{2+} with Al^{3+} in the spinel layer of BAM proceeds in a fashion analogous to the replacement of Mg^{2+} with Al^{3+} in normal spinel ($MgAl_2O_4$). This is most readily seen if the compositions along the BAM–BAL join are described on an O_{16} basis in the spinel block, i.e., as $BaO \cdot MgAl_{10}O_{16}$ (BAM) and $0.727BaO \cdot Al_{10.67}O_{16}$ (BAL), as in Eq. (1). Note that this leads to a very straightforward description of the solid solution: 1 Mg atom is replaced by 2/3 of an Al in each cell (as is required for charge balance), and some BaO is removed from the cation layer.

In BAM, the composition of the spinel layer is given by $MgAl_{10}O_{16}$. According to Eq. (2), this would set $y = 0.75$, leading to a formula of $(Mg_1Al_3)^{IV}(Al_7\square_1)^{VI}O_{16}$ (if we multiply by 4). In fact, this expression exactly describes the observed structure and stoichiometry of the spinel units in BAM: one tetrahedral Mg, 3 tetrahedral Al and 7 octahedral Al in a close packed array of 16 O atoms [7]. Finally, if we combine this expression with Eq. (1) we come to a complete description of the BAM–BAL join as a function of our compositional variable, x:

$$(1-\tfrac{1}{4}x)BaO \cdot (Mg_{1-x}Al_{3+x})^{IV}(Al_{7-(x/3)}\square_{x/3})^{VI}O_{16}. \quad (3)$$

Note the slope on the BaO in Eq. (3) has been changed from −3/11 to −3/12 (or −1/4), in order to make it consistent with the crystal structure of BAL. Regarding this, the authors point out that in the original crystallography work of Iyi et al., density, cell volume and microprobe analysis determined a composition for BAL of $Ba_{0.79}Al_{10.9}O_{17.14}$, as opposed to $Ba_{0.75}Al_{11}O_{17.25}$. On an O_{16} basis this other stoichiometry corresponds to a composition of $0.77BaO \cdot Al_{10.67}O_{16}$. In addition, it is known that there is a modest solid solution domain around BAL on both the BaO and Al_2O_3 rich sides [13]. Therefore, it is reasonable to suggest that the slope on the BaO in Eq. (3) be −3/12. It is also important to point out that this model is consistent with prior descriptions of the crystal structure of BAL. The loss of BaO from the cation layer clearly must be accompanied by a local structural rearrangement (there is not going to simply be a void of atoms in that cell). Previously, this has been described as the removal of Ba, with the addition of interstitial oxygen and the formation of Al_i–O_{Ba}–Al_i bridges [8–10]. What is being accounted for in either description is that one out of every four formula units in the lattice is replacing the Ba–O layer with a structure that resembles a stacking fault in spinel. In this picture, then, the evolution of the crystal structure from BAM to BAL is readily described in the following way: (a) tetrahedral Mg^{2+} is replaced by Al^{3+} in the spinel layer, with the formation of octahedral Al^{3+} vacancies in 1/3 of the formula units, (b) four formula units containing $(MgAl_3)^{IV}$ become four units containing $(Al_4)^{IV}$; in one of these four formula units a spinel stacking fault structure is created, replacing the Ba–O cation layer of that unit. This model assumes that no Mg is present on octahedral sites. Recent Rietveld refinements on BAM indicate that this is a reasonable assumption [23].

Based on this model, there are two potential assignments for the EuIII emission in these materials. That is, there are two types of crystal defects that may form as the composition is changed from BAM to BAL, either one of which may cause a change locally from an EuI center to an EuIII center. One is the assignment of Stevels, that the Eu^{2+} ions associate with O atoms in the cation layer to form a new Eu^{2+}–O_{Ba} center [11]. The second possibility is that a new center is formed by Eu^{2+} atoms in formula units near Al^{3+} octahedral vacancies. Such vacancies are expected to create additional electron density directed toward Eu^{2+}, an effect that should red shift the Eu^{2+} emission [25], creating the peak at 538 nm. We have attempted to model each of these possibilities on a purely statistical basis, i.e., we have calculated the predicted ratio of EuIII sites to "normal" sites (BR or a-BR sites) as a function of the composition variable x, based on the assumption that the distribution of defects and the distribution of Eu^{2+} are both completely random within the host. The difficulty with

the first case is that in BAL there are no pristine BR sites left in the lattice—each Ba site in a formula unit is at least corner-sharing with an O_{Ba}, and many are in contact with several O_{Ba}. Thus, some arbitrary decision would have to be made as to which arrangements generate an Eu^{2+}–O_{Ba} center.

For the case in which EuIII is assigned to a site near an Al vacancy, the relative site populations can be calculated directly. The absolute emission intensities from these sites are not expected to directly quantify site populations due to possible differences in efficiency; however, the observed ratios of these emissions can give us an idea of the expected trend in site populations with composition. Therefore, we have calculated the ratio of the integrated emission intensities, EuIII/(EuI + EuII), for each composition based on our peak fitting work, and compared it to the ratio predicted by Eq. (3) according to our assignment of the different centers. In this model we assumed a random distribution of Eu atoms, and also assumed that two Al^{3+} vacancies will not occur in the same formula unit. EuI and EuII were taken together in the calculation because the model makes no predictions about the relative amounts of Eu^{2+} on BR and anti-BR sites. The data are shown in Fig. 10. The model provides a reasonable fit to the observed trend in emission ratios. However, the observed population of EuIII does not increase as rapidly as is predicted by the model. This suggests that the distribution of Eu^{2+} ions is not random, but that Eu prefers to avoid sites near defects in the lattice.

In fact, this preference is easily seen when BAL is doped at different Eu concentrations. Normalized emission spectra for BAL at 1%, 5% and 10% Eu^{2+} are shown in Fig. 11. It is clear from the spectra that the three sites are not populated evenly—the EuIII site appears to be the last center to be populated as the concentration is increased. Even so, we do not believe

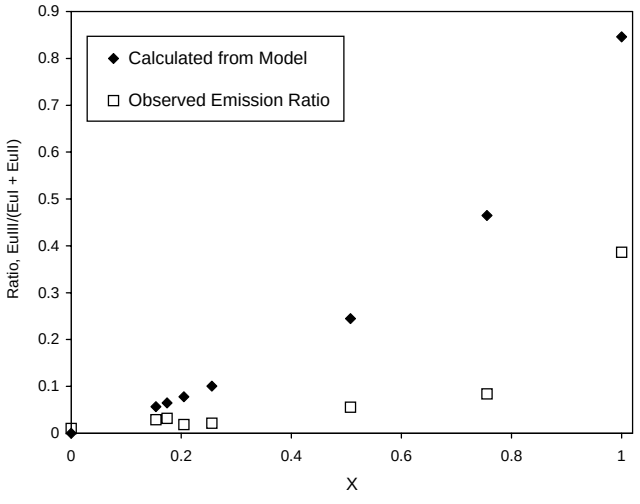

Fig. 10. Emission intensities predicted by Eq. (3) (closed diamonds) compared to those calculated from peak fitting data (open squares).

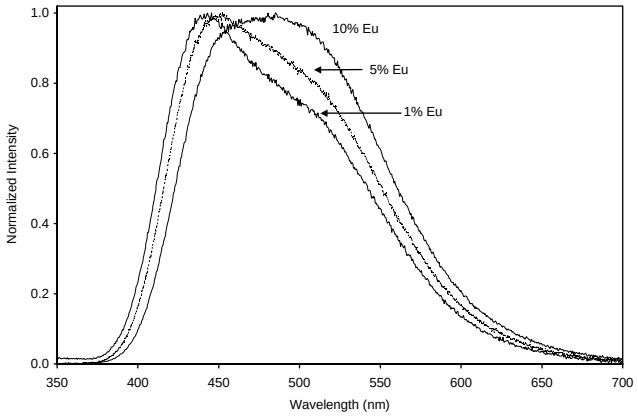

Fig. 11. Normalized emission of BAL doped at 1%, 5% and 10% Eu ($\lambda_{ex} = 147$ nm).

that enough evidence has been gathered to favor one assignment over another. We are currently studying the effects of VUV radiation damage on these materials. The results of this study may help clarify the assignment of the EuIII center.

4. Conclusions

The solid solution between BAM and BAL has been characterized using VUV excitation, emission and reflectance spectroscopy. Replacement of Mg^{2+} with Al^{3+} in the lattice results in a significant broadening of the Eu^{2+} emission as well as a decrease in efficiency. The defect chemistry of this solid solution has been modeled using the known defect chemistry of spinel. Changes in the composition of the material are accompanied by the formation of Al^{3+} octahedral vacancies, and the random replacement of 1/4 of the Ba–O layer with Al_i–O_{Ba}–Al_i stacking faults. The changes in the emission spectra have been associated with changes in the relative populations of Eu centers in the host using this model, whereby Eu^{2+} occupies BR and anti-BR sites, and a third site that is either an Eu^{2+}–O_{Ba} center or an Eu associated with nearby Al^{3+} vacancies in the spinel layer. Finally, evidence has been presented that under VUV excitation, energy transfer to Eu^{2+} in BAM may proceed via a broad exciton emission of the host centered at 263 nm.

Acknowledgments

Dr. Diaz thanks Research Corporation Cottrell College Science Awards, OSRAM SYVANIA Inc., and the Faculty Research Fund of Central Washington University for support for this work. The authors also thank Dr. Robert McSweeney for the preparation of samples for this study, and for helpful discussions.

References

[1] A.L. Diaz, B.G. DeBoer, C.F. Chenot, 19th International Display Research Conference Proceedings, 1999, pp. 65–68.
[2] S. Oshio, T. Matsuoka, S. Tanaka, H. Kobayashi, J. Electrochem. Soc. 145 (1998) 3903.
[3] H. Bechtel, T. Jüstel, H. Gläser, D.U. Wiechert, J. SID 10 (2002) 63.
[4] M. Ushirozawa, SID Digest (2000) 224.
[5] S. Zhang, M. Kokubu, H. Fujii, H. Uchiike, J. SID 10 (2002) 25.
[6] M. Göbbels, S. Kimura, E. Woermann, J. Solid State Chem. 136 (1998) 253.
[7] N. Iyi, Z. Inoue, S. Kimura, J. Solid State Chem. 61 (1986) 236.
[8] N. Iyi, Z. Inoue, S. Takekawa, S. Kimura, J. Solid State Chem. 52 (1984) 66.
[9] F.P.F. van Berkel, H.W. Zandbergen, G.C. Verschoor, D.J.W. Ijdo, Acta Cryst. C 40 (1984) 1124.
[10] J.-G. Park, A.N. Cormack, J. Solid State Chem. 121 (1996) 278.
[11] A.L.N. Stevels, J. Lumin. 17 (1978) 121.
[12] C.R. Ronda, B.M.J. Smets, J. Electrochem. Soc. 136 (1989) 570.
[13] B.M.J. Smets, J.G. Verlijskonk, Mater. Res. Bull. 22 (1986) 1305.
[14] T. Jüstel, H. Nikol, Adv. Mater. 12 (2000) 527.
[15] K. Yokota, S.-X. Zhang, K. Kimura, A. Sakamoto, J. Lumin. 92 (2001) 223.
[16] P. Boolchand, K.C. Mishra, M. Raukas, A. Ellens, P.C. Schmidt, Phys. Rev. B 66 (2002) 134429.
[17] K.C. Mishra, M. Raukas, A. Ellens, K.H. Johnson, J. Lumin. 96 (2002) 95.
[18] A. Ellens, F. Zwaschka, F. Kummer, A. Meijerink, M. Raukus, K. Mishra, J. Lumin. 93 (2001) 147.
[19] T. Jüstel, J.-C. Krupa, D.U. Weichert, J. Lumin. 93 (2001) 179.
[20] B. Henderson, G.F. Imbusch, Optical Spectroscopy of Inorganic Solids, Oxford Science Publications, Clarendon Press, Oxford, 1989 (Chapter 5.4).
[21] C.W. Struck, W.H. Fonger, Understanding Luminescence Spectra and Efficiency Using Wp and Related Functions, Springer, Berlin, 1990.
[22] V.T. Gritsyna, I.V. Afanasyev-Charkin, V.A. Kobyakov, K.E. Sickafus, J. Am. Ceram. Soc. 82 (1999) 3365.
[23] Y.-I. Kim, K.-B. Kim, M.-J. Jung, J.-S. Hong, J. Lumin. 99 (2002) 91.
[24] A.M. Srivastava, J.F. Ackerman, W.W. Beers, J. Solid State Chem. 134 (1997) 187.
[25] A.L. Diaz, D.A. Keszler, Chem. Mater. 9 (1997) 2071.